2015 IEEE International Conference on Robotics and Automation (ICRA)
Washington State Convention Center
Seattle, Washington, May 26-30, 2015

Simplified Adaptive Path Planning for Percutaneous Needle Insertions*

Éderson Dorileo, Abdulrahman Albakri, Nabil Zemiti, Philippe Poignet

Abstract— **Needle placement errors can mitigate the effectiveness of the diagnosis or the therapy, sometimes with catastrophic outcomes. Previous design of a simplified model for needle deflection estimation was motivated by the clinical constraints of ARCS (Abdomino-pelvic Robotic-driven slightly flexible needle insertion performed in CT/MRI-guided Scenario). We present in this work, the validation results for the needle deflection prediction model. Its robustness is evaluated under an unknown context such as a different robotic platform, facing uncertainties conditions not conceived previously in the model´s confection. In addition, the work presents the development and validation experiments of an adaptive path planner that uses the model as predictor's strategy. It provides pre-operative planning assistance, as well as intra-operative decision-making support. The experiments results showed average error around 1mm for the pre-operative planning and the intra-operative replanning approach showed to be very robust to correct the initial predictions, showing average error smaller than 1 mm.**

I. Introduction

Image-guided percutaneous needle insertion is a challenging minimally invasive procedure largely used under medical diagnoses and treatments such as drugs delivery, tumor ablation or biopsy. Often, the target can´t be achieved and the needle has to be reinserted, meanwhile the failure rates can reach until 30% of the cases, depending on the procedure complexity [1]. Moreover, errors in needle placement can mitigate the effectiveness of the diagnosis or the therapy. For example, this leads to false negatives during biopsies or destroys healthy instead of cancerous tissue in brachytherapy, sometimes with catastrophic outcomes [2].

According to what has been described in several studies, the needle deflection is specially associated with the geometry of the needle tip and the mechanical properties of the tissue [3]. Typically, the needle passes through tissues of varying densities, which make it deflect. Past works have shown that straight needle trajectory is not sufficient for precise targeting since needles can deviate slightly from a straight-line path due to tissue deformation or inhomogeneity [4]. However, most of the current insertions in the clinical routine applications, take the line as reference due to its simplicity or environment´s constraints.

In this paper, we present a new planning method for percutaneous insertions that uses a simplified needle's deflection prediction model in order to minimize the reinsertion trials or other errors that could compromise the intervention´s success. The algorithm design was motivated by the clinical demands of ARCS (Abdomino-pelvic Robotic-driven slightly flexible needle insertion performed in CT/MRI-guided Scenario) targeting biopsies of kidney. The planner provides pre-operative assistance in order to optimize the insertion point. In addition, the intra-operative (online) adaptive replanning provides decision-making support considering changes in the path due to the environments' uncertainties. The adaptive algorithm allows the planner to improve its own performance under uncertainties conditions, such as tissue deformation, tissue inhomogeneity, topological changes of the tissue and other modeling approximations. The simplified adaptive path planning has the quality of absorbing the advantages of the model, such as simplicity and ARCS compatibility. Our approach was developed under the context of the ANR-ROBACUS project. The referred project is committed to the improvement of the 6-Dof LPR (Light Puncture Robot), developed by TIMC-IMAG – University Joseph Fourier, France. The robot integrates a CT/MRI compatible patient-mounted teleoperated platform [5] designed to perform abdominal and thoracic punctures [6] [7].

For simplicity's sake, in this study we used Raven platform instead of the preconized LPR. It prevented us to compete for the access of scarce clinical resources, such as CT/MRI machines. It also allowed us to evaluate platform independence of our approach. Therefore, its robustness is showed under the uncertainties of an unknown scenario, facing conditions not previously conceived in the model's confection (*e.g.,* outside tissue needle bending: in LPR, it is not significant, since the grippers were designed to be close to the insertion point).

II. Related Work

Needle motion planners have been designed in the aim of guiding robotic-driven interventional procedures by modeling needle deflection due to the tissue interaction. However, according to Misra *et al*. [8], needle path planning procedures require an accurate model of the needle-tissue interaction. They showed how the needle deviation during insertion can be described using energy-based approach and how the needle-tissue interaction and the transverse force in the needle tip holds 99.9% of the stored strain energy during the needle insertion. Euler-Bernoulli cantilever beam and extensions of its theory has been used to compensate pre/intra-operatively for needle deflection [9]. In ref [9], the needle is modelled as a flexible beam with clamped support at one end, being its deflection estimated using online force/moment measurements at the needle base. The needle deflection compensation is performed by axial needle rotation through 180°. Intra-operative computation of needle

*Research supported by ANR (National Research Agency - France) in the context of the TECSAN project ROBACUS (ANR-11-TECS-020-01).

The authors are with LIRMM – Robotics Department, University Montpellier II, France. (e-mails: {name.surname}@lirmm.fr).

deflection and steering was presented in [10], in which a linear beam supported by virtual springs was used to estimate the system´s parameters using a real-time (RT) fluoroscopic guidance designed for flexible needles.

Several studies have examined the use of nonholonomic path planning algorithms for robotic-driven needle insertions. Main existing works have been committed to provide pre/intra-operative decision-making support [11] [12] or delivering important skills such as needle steering [3]. However, according to Kobayashi *et al.* [11], in many percutaneous therapies, the needle path is limited and has some constraints imposed by the abdominal wall. They underlined that the needle steering methods, which have been discussed in many previous works [3] [10], cannot be used in many cases because of needle stiffness. *I.e.,* needles used in abdominal insertions are semi-rigid (slightly flexible). Therefore, they provided a planning method to decide robust paths of straight needle insertion for various puncture points. Their approach considers a probability-based puncture condition, followed by a definition of the expected value of the needle placement accuracy. The numerical simulation optimization method searches pre-operatively the insertion path in such a way that minimizes the needle placement error. In-vitro experiments showed needle insertion with a mean accuracy of 1.5 mm.

Dehghan et al. [12] proposed an iterative optimization method to optimize the needle insertion entry point, heading and depth for needle insertion, while minimizing the distance between a number of specified targets and the needle. The deformable tissue is described by a finite element method while the neo-Hookean material model is exploited to determine the effects of geometric and mechanical non-linearities and compressibility effects. The simulation-based optimization algorithm is shown converging in few iterations and decreasing the targeting error effectively under the prostate brachytherapy simulator.

ARCS has special challenges associated to the bore size, radiation and ferromagnetic compatibility. The singular complexity of this scenario make difficult to incorporate most of the existing needle deflection modeling approaches not originally conceived for this context. In order to give an example, in most of the cases, the intra-operative use of conventional force sensors is not possible in the clinical routine concerned to ARCS. Hence, the direct application of the classically known approaches [10] [13] is limited as well.

III. The Simplified Model

The proposed Simplified model´s design is a function of the needle (*Kn*) and tissue (*Kt*) properties (stiffness), as well as needle tip asymmetry (α). We assume that the semi-rigid needle performs small-deflections, (if comparable with nitinol needles), in accord to the small-deflection beam theory $(\Delta x/\mathrm{L} < 0.1)$[14]. L is taken as the needle length (distance AB between the end-effector and the needle tip) projected along the y axis and *Δx* is the amount of deflection orthogonal to the insertion. We also assume that the needle tip deflects in the direction of the bevel due to the asymmetric forces acting on the needle tip (Fig. 1). Therefore, the resultant force $\vec{F}_R$ represents the sum of all the

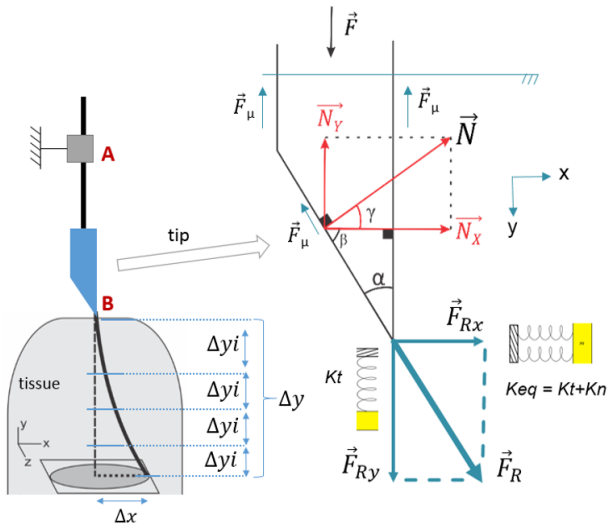

Figure 1. Insertion of a semi-rigid needle into a soft tissue. The simplified model considers deflection in the direction of the beveled tip, assuming a sequence of intermediate displacement.

forces actuating on the system, in particular the input force $\vec{F}$ and friction force $\vec{F}\mu$.

Therefore, the resultant force $\vec{F}_R$ represents the sum of all the forces actuating on the system, in particular the input force $\vec{F}$ and friction force $\vec{F}\mu$.

The derived expressions concerns the dynamics of the needle during the insertion into an elastic body and describe the relationship between the normal ($\vec{N}$) and the resultant ($\vec{F}_R$) force components acting on the needle as shown in Fig. 1. The analysis takes *Kt* as the tissue stiffness at the needle tip, and assumes that the resultant component in the *x* axis ($\vec{F}_{Rx}$) can be represented by parallel springs and the stiffness of each spring is given by the needle (*Kn*) and tissue (*Kt*) stiffness. The needle axial deformation is negligible compared to the tissue deformation. It allows us to represent the resulting y-component by a single spring with stiffness *Kt*. Therefore, we have that

$$\vec{F}_{Rx} = (Kn + Kt) * \delta x \tag{1}$$

and

$$\vec{F}_{Ry} = Kt * \delta y \tag{2}$$

In the relationship presented below (3), the system's dynamic analysis during the insertion is considered. $\vec{F}_{Rx}$ acts transversally and causes needle deflection, while $\vec{F}_{Ry}$ is the axial force that allows the needle to be displacement in the y axis. Transversal and axial forces are observed in the relationship with each component of the normal force acting in that direction.

$$\vec{F}_{Rx}/\vec{N}_x = \vec{F}_{Ry}/-\vec{N}_y * H \tag{3}$$

An adaptive parameter (H) was conceived as the slop in the relationship between the normal force and virtual springs actuating in the needle tip. Its initial value was heuristically set as (H_0=0.02). This value represents the magnitude order between the axial and transversal components of the model, taking into account the properties of the needle and tissue. Using (5), H is updated, for each insertion step, according to the needle tip position measured from the images. This update works as a failure contingence mechanism and allows online correction regarding to the error $(e_i = \Delta x_i - \Delta x'_i)$ between the predicted deviation at that insertion step (Δx_i) and the needle tip deviation observed ($\Delta x'_i$) from the image. The update, for each insertion step i, is performed according to:

$$H_{i+1} = H_i(\Delta x_i + e_i) \quad (4)$$

The study of the normal force in the needle tip (Fig. 1), gives us that the angle γ is the same one as in the beveled needle tip (γ=α). Then, having $\vec{N}x = cos(\alpha) * \vec{N}$ and $\vec{N}y = sin(\alpha) * \vec{N}$ and from (1), (2) and (3), we can write the deflection orthogonal to the insertion as:

$$\Delta x_i = \frac{cot(\alpha) * Kt_i * \Delta y_i * H_i}{(Kt_i + Kn_i)} \quad (5)$$

The tissue (stiffness) parameters (Kn) can be obtained pre-operatively, using MRI or US elastography [15] [16], for example. Otherwise, tissue parameters at surface level can be obtained by axial compression tests as in ref [10] or using suction light pipettes as in ref [17]. Then, the errors due the initial tissue properties measured at surface and tissue inhomogeneity along the needle shaft are incorporated in the online correction. H is updated intra-operatively, according to the position feedback obtained from the needle tip images. The Simplified model doesn´t requires force sensor input and has the advantage to be simple in the sense that it demands a few number of parameters and it is compatible to ARCS scenario.

IV. Adaptive Path Planning

Motion planning algorithms can compute feasible trajectories for systems, with some additional coverage of feedback and optimality. According to LaValle [20], some basic components arise throughout virtually all of the topics covered as part of planning: a) Time; b) Actions; c) Plan; d) Criterion and e) State. The link of our work with these basic components will be discussed in this section in the aim of supporting the characterization of our approach under the theoretic context of adaptive path planning.

(1) Time: For this study, we consider that the system can work under interactive (asynchronous) time or under synchronous time. For the first case, each decision can be taken only after the previous process is over. It usually happens in ARCS, in which the CT/MRI machine can take around 4s to update and reconstruct the workspace under 3D imaging. On the other hand, the synchronous time occurs, for example, when regular insertion intervals are defined before start the insertion. It is the case for the experiments setup designed for this validation study. **(2) Actions:** Actions are generated by the plan and can manipulate the state. The main actions specified to the planner developed in this work are: estimateEntryPoint(), simplifiedPathPlanning() and adaptiveReplanning(). They are discussed in details in the next topic, as well as, how the state changes when actions are applied. **(3) Plan:** In our study, the predictor's strategy imposed to the path planner is the following up of the needle tip deflection behavior, modeled by the Simplified model. It can predict future states of the insertion procedure, while allows to the planner performing intra-operative replanning assistance. Considering the clinical demands of ARCS scenario, for each insertion step, intra-operative decision-making support can guide the user in order to avoid future predicted damages. Therefore, two main reactive plans are possible: a) perform needle insertion (authorize next insertion step); or b) withdraw the needle (procedure aborting followed by insertion retrial), in case of the planner indicate that continuing the needle insertion could be unsafe to the patient or compromising the success of the procedure. **(4) Criterion:** The algorithm´s design works under the concept of optimality. I.e., in addition to arriving in a goal state, the planner is able to modify its own operation in order to achieve the best possible mode of operation. It is a very useful skill when facing uncertainties of the medium. **(5) State:** We proposed a state machine composed from an initial and a goal state, having as intermediate states: the pre-insertion planning, the intra-insertion replanning and the idle state. We will describe bellow how the planner goes through these states considering the main actions required by the clinical scenario in ARCS.

The procedure starts when the user defines the target position. At this moment, we start the pre-insertion planning state, which is defined as the moment before the needle touching the tissue. A sequence of actions allows the system to switch to idle state and back again. Idle is the state in which the planner is basically waiting for user's decision or robot-driven needle movement. For example, as soon as the target is defined, the system can estimate the optimal needle entry point (estimateEntryPoint) for the current procedure. Once the robot places the needle in the scenario and it is ready to start the insertion, the user can confirm manually the position of the needle tip. Then the system runs the simplifiedPathPlanning algorithm, meaning the initial path planning that will be performed pre-operatively. As soon as the robot starts the needle insertion, the planner starts the intra-insertion (online) replanning state, in which a loop of actions runs until that the system reaches the goal state.

In short, as mentioned before, for each insertion step, the user/system updates needle tip position. Then, the system replans the path previously planned (adaptiveReplanning). The main algorithms mentioned here, as well as, how the Simplified model (calcDeflection) was embedded in the planner, are presented in details in the Algorithm 1.

V. Problem Definition and Formulation

We report two main goals in this work: a) Simplified model validation for needle deflection prediction under unknown scenarios (P1). b) Simplified adaptive motion planner design and validation (P2). For both definitions, references about pre-operative (P) computing is related to the moment before the needle tip touching the tissue; while

Algorithm 1: Simplified Adaptive Path Planning

```
Point estimateEntryPoint ( pBase, pEntry, Δy )
    1: pLinear ← simulateLinearPath( pBase, pEntry, Δy )
    2: Δx ← calcDeflection( Δy , Kn, Kt, α )
    3: pEntry ← correctPEntry( pLinear , Δx )
    4: return pEntry
Vector<Point> simplifiedPathPlanning ( pBase, pEntry, pTip, Δy )
    1: for each ζ < Δy do
    2:     pLinear ← simulateLinearPath( pBase, pEntry, Δy(ζ) )
    3:     Δx(ζ) ← calcDeflection(Δy(ζ) , Kn, Kt, α, H )
    4:     T.add( pLinear, Δx(ζ) )
    5: return T
Vector<Point> adaptiveReplanning ( pBase, pEntry, H )
    1: ψ ← updateTipPosition()
    2: Δ ← calcDistanceFromReferenceLine(ψ)
    3: Δx(ζ) ← simplifiedPathPlanning ( pBase, pEntry, ψ, Δy(ζ) )
    4: H ← updateAdaptiveFactor( ε(Δx(ζ).back(), Δ), H )
    5: return H
```

online (O), refers to the intra-operative time, when the insertion procedure is in-operation and the needle tip is inside of the tissue. In this section, we discuss how each of these orientation problems were formulated and how they guided the experiments design and the result's analysis.

A. *Simplified Model Analysis (P1)*

The goal defined by this analysis is stated according to: **Problem 1 (P1):** "What is the model's error while simulating needle **tip** deflection behavior regarding to a **linear** path?"

The Simplified model validation is analyzed according to the simulation of needle deflection orthogonal to the insertion direction (Δx). The simulation is performed pre-operatively (P) and online (O). This problem formulation leads us to explore the relationship between the needle tip position observed from the image (N) and the segment ($\overline{DEL}$), concerning to the linear insertion direction. Therefore, the validation proposed under this analysis takes in to account (P) and (O) estimations of (Δx), having as reference the linear direction (L). Also, in order to obtain the desired error according to P1 definition, the needle itself (N) might to be taken as reference in the analysis. The scheme presented in the Fig. 2A, illustrates the analysis according to P1.

B. *Adaptive Path Planning Analysis (P2)*

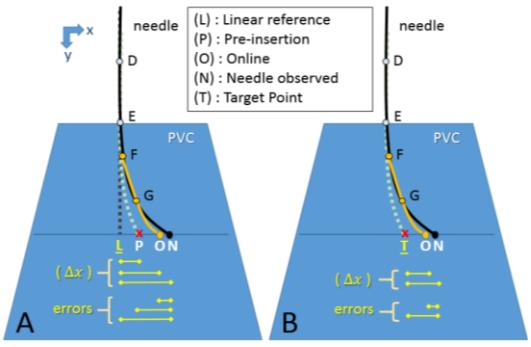

Figure 2. Out of scale illustration scheme of the problem's formulation and analysis. A. Simplified model analysis (P1). B. Adaptive path planning analysis (P2).

The aim of this validation can be stated according to the

Problem 2 (P2): "What is the planner´s error while predicting how far the needle **tip** will be from the **target**?"

The analysis of the simplified adaptive path planning was motivated by the clinical demands of ARCS. Therefore, from now on, the pre-insertion (P) simulation has the meaning of the target point (T) (and the associated path to reach it). It means that, if the needle is inserted in the predicted entry point (E), then (P = T); and the needle should reach the target as illustrated in the Fig. 2B. The motion planner also considers that due to the uncertainties of the medium, the actual path of the needle could deviate of the initially planned path. Then, during the insertion, the online (O) algorithm replans the previously planned path (P) to be as fit as possible of the actual needle path. The performance quality in this fitting strategy will allow to the user the best decision making during the insertion, enhancing the procedure safety and avoiding future (predict) damages.

Therefore, the preconized analysis on this time would explore the relationship between the observed needle tip (N) and its distance (Δx) from the online (O) replanning, as well as the referential target point (T). Again, in order to obtain the desired error according to P2 definition, the needle (N) might to be taken as reference in the analysis. The scheme presented in the Fig. 2B, illustrates the analysis according to P2. The observation of the study available in the Fig. 2 shows that P2's errors analysis is very similar to the error's analysis formulated in P1.

VI. Experiments Setup

The experiments were performed using the cable-driven (6 DOF + grasp) Raven II robot platform, developed by the University of Washington (Surgical Robotics) [19]. It is a state-of-art open architecture (software & hardware) surgical robotic system for surgery research. Its Linux-based operating system allows modifications and improvements of the original code, creating a way for researchers to experiment and collaborate. For the needle insertion experiments, the robot tools were removed and a customized adapter was built in order to fix the base of the needle and a force sensor device in the robot's arm (Fig. 3).

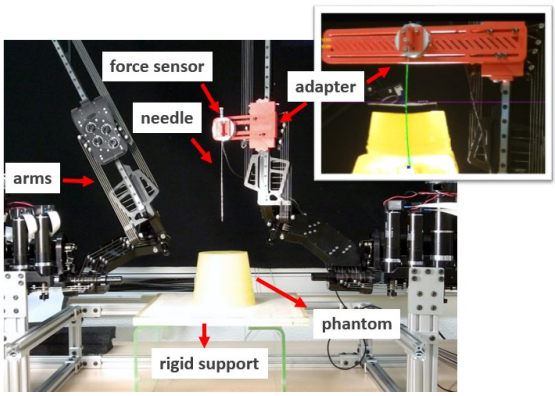

Figure 3. The open-source Raven robot. Original platform was customized in order to perform needle insertion experiments.

A long (20 cm), 17 degrees bevel-tip spinal needle was inserted in three different types of synthetic phantom tissues: a) homogenous 100% soft PVC phantom; b) two-layers phantom: very soft PVC (80% soft PVC + 20% plastic softener) + medium density PVC (70% soft + 30% hard PVC); c) four-layers phantom: (synthetic leather, sponge, soft and hard PVC). This last one intended synthetically reproducing the multi-layer medium usually found in the clinical procedures, such as: skin, fat, mussels and organ.

Video images (1920 x 1080 px) were acquired using a digital video camera Toshiba Camileo Z100 and measurements of the scenario were recovered thanks to accurate camera calibration using planar fiducials markers [20]. The needle was visually detectable because the tissues used were translucent. The track of the needle's position was performed manually. It was done by using a single mouse's click in the interactive GUI.

The insertions were performed progressively, with regular intervals defined pre-operatively. The velocity was of 0.03 m/s and, for each insertion step, pauses of 7s were defined in order to wait for tissue relaxation (Fig. 4), followed by manual needle tip position update. For homogeneous tissue, we also observed the system's behavior under insertion velocity of 0.06 cm/s. In general, for each experiment, there were two pauses, considering insertion depths between 6 and 10 cm. For issue of this validation study, 44 insertion samples were performed using a digital 12Mpx video camera. A 6-DoF force-torque sensor (nano43 / SI-36-0.5 / ATI Industrial Automation) was attached to the robot´s arm and it was used to record the resulting forces and torques of the system. The force data were used as ground truth and also to enrich the system's study and observations. They were not considered as input in the modeling. Stainless (316) steel 18-gauge needle was used having an outer diameter (*do*) of 1.27 mm and an inside diameter (*di*) of 0.838 mm. It exhibits 193-GPa Young modulus (E) [10] and moment of inertia $I = \pi/64*(do^4 - di^4) = 0.103$ mm^4. The needle stiffness is given by $Kn = 3EI/L^3$, being L the needle length. The tissues properties were preoperatively estimated by axial compression test at tissue surface level as in ref [10], having the coefficients *Kt*(Homog)=490 N/m, Kt(2Layers)=115 N/m and Kt(4Layers)=130 N/m.

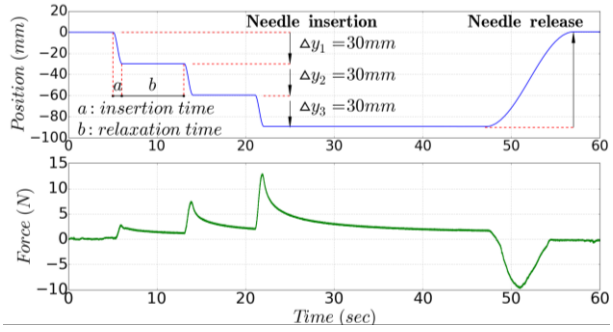

Figure 4. Position and Forces recorded during the percutaneous insertion procedure under homogeneous tissue (V=3cm/s).

VII. RESULTS

We experimentally evaluated our approach under applications involving the simplified adaptive path planning approach motivated by the ARCS scenario demands. We now present the validation results obtained using the definitions and setup presented in the previous section. First, we analyzed the needle's deflection prediction model in the deviations orthogonal to the insertion direction (linear reference), according to the P1 formulation (section V.A). The Fig. 5 presents the deviations of (P), (O) and (N), (ref. Fig. 2.A) relating them to the insertion depth, considering the set of experiments. From the linear regression, we observe that for small depth of insertions, (O) is closer to the actual needle observations (N), while (P) has its performance quickly improved with the needle insertion depth increasing. This observation reveals that the prediction model has its intra-operation simulation ability (O) very dependent to the insertion depth.

It´s possible to see in the cloud of points the definition of two clusters thresholded by the point where (P) cross (O), around 70 mm of insertion depth. The presence of these clusters suggests the importance to use (O) and (P) simulations concomitantly, since the results show that they are very complementary in their performances. For example, the performance analysis of (P) for deeper insertions reveals the importance of getting high accuracy in the insertion point definition. It could part of a very efficient strategy to enhance the safety of percutaneous insertions procedures by avoiding damages caused by reinsertions trials or by excessive intra-operative corrections interventions.

Secondly, we analyzed the adaptive path planning motivated by the formulations of P2. The Fig. 6 shows the distances observations motivated by this analysis. Having the target point as referential, this analysis shows how trustable is the motion planner while providing intra-operative (O) decision-making assistance. We observe the linear regression lines slowly diverging according to the insertion depth. However, the planner shows to be very robust for (O), keeping its distance from the actual needle in less than 1 mm, even for the deeper insertions.

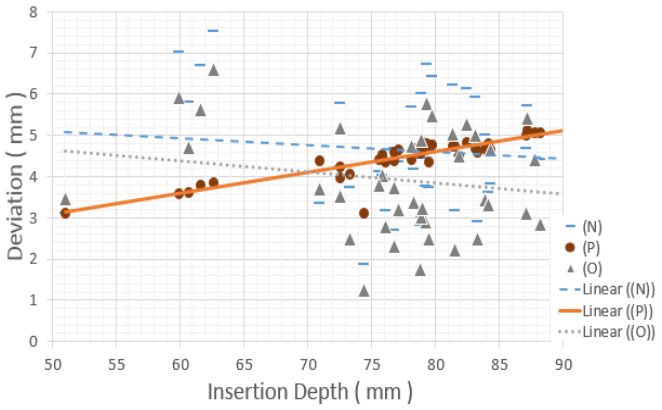

Figure 5. Simplified model validation analysis. Deviations observations under linear referential, according to P1 formulation.

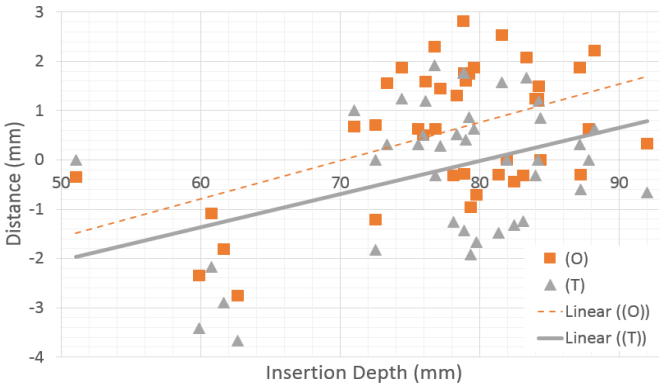

Figure 6. Online adaptive path planning validation analysis. Distance study motivated by P2 formulation.

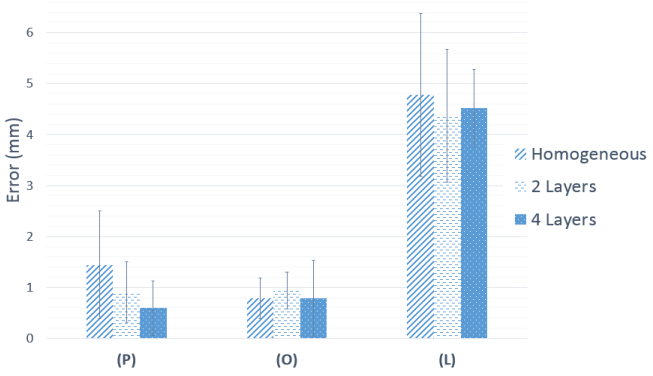

Figure 7. Errors according to P1 and P2 formulations, for the several mediums.

Errors according to P1 and P2 formulations are presented in the Fig. 7. The graphs show the analysis taking as reference the actual position of the needle tip. The errors quantification is summarized in the Table I.

TABLE I. SUMMARY OF THE QUANTIFIED ERRORS ACCORDING TO (P1) AND (P2)

	P (mm)	O (mm)	L (mm)
Homogeneous	1.44 ± 1.05	0.78 ± 0.40	4.78 ± 1.60
2 Layers	0.90 ± 0.59	0.94 ± 0.36	4.37 ± 1.3
4 Layers	0.59 ± 0.55	0.79 ± 0.55	4.52 ± 0.92

Insertion depths average for homogeneous, two-layers and four-layers phantoms were nearly: 73 mm, 78 mm and 86 mm. The pre-operative path planning algorithm (P) had the average error around 1mm and showed good performance for deeper insertions, even under complex mediums insertions (e.g. four-layer tissues).

The online replanning approach (O) showed to be very efficient to correct itself, overcoming the scenario´s uncertainties and model´s approximations during the procedure.

The Fig. 8 shows insertion sample under homogeneous tissue. The insertion sequence illustrates initial path planning performed pre-operatively (P) (Fig. 8B). A sequence of intra-operative (O) path updates (Fig. 8D-F) is performed during the insertion. Then, the Fig. 8H-I show how the system can adapt itself in order to provide a better estimation of the final needle tip position.

The system's behavior for insertions under different velocities, was registered considering similar insertion depths. For this experiment, we observed that the bigger is the velocity, less the needle deviates from the (linear) insertion direction. *I.e.,* the needle deflection presented an inverse relationship regarding to the velocity of insertion. However even considering this important change in the system's behavior the path planning was robust and stable enough to predict the final needle deviation under submillimetric precision.

VIII. CONCLUSION AND FUTURE WORKS

In this work, we presented the development and validation of a simplified adaptive path planning. Its design was motivated by the constraints of ARCS scenario. The planning algorithm uses the simplified needle prediction deflection model embedded in its strategy and can provide pre-operative planning assistance, as well as, intra-operative (online) decision-making support. The prediciton model and

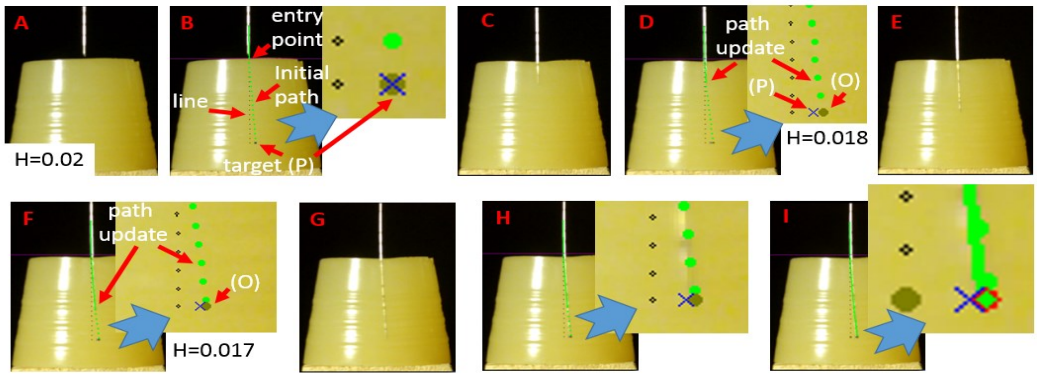

Figure 8. Insertion sequence showing pre-operative planning (P) and intra-operative (online) replanning. The adaptive factor (H) updates the expected path and position of the needle (O) for each insertion step.

motion planner algorithm were validated according to the P1 and P2 formulations that guided the experiments design and result's analysis.

The deviation analysis of the model showed good performance for the pre-operative simulations, especially for deeper insertions. The distance analysis showed error smaller than 1 mm for motion planner under intra-operative replanning. Its robustness and consistence were observed when comparing the errors obtained for the several tissues used in the experiments, as well as, when comparing the results considering similar tissues. The approach showed to be very robust when facing the unknown scenario and when adapting itself regarding to the environment's uncertainties.

Our approach has the advantage to be simple and compatible to ARCS. Moreover, it allows appropriated user's action during the procedure, even for the cases where the needle tip is not visible or not available. *E.g.*, RT 3D CT/MR imaging scenarios. It provides useful information at the appropriate moment in order to aid decision-making and enhancing safety in ARCS procedures. For example, in the cases where the needle tip is not visible or not available in RT (e.g. 3D CT/MRI), our planning strategy could enable the appropriated clinical action by supplying simulated feedback of the current needle tip position.

In future work, this approach will be tested, considering the extension of the algorithm to the 3D environment, *i.e.,* under the CT/MRI scenario. Finally, we plan to evaluate our approach motivated by needle steering applications in non-homogenous soft mediums experiments. The simplicity and fast computation makes it suitable for online 3D needle steering, considering, for example, the angle of the needle when moving its base.

REFERENCES

[1] C. Fouard, A. Moreau-Gaudry, N. Zemiti and P. Poignet, "Light robot for the tele-operated needle insertion with physiological movements compensation," ANR-TECSAN - Technologie pour la santé et l´autonomie: The ROBACUS project, Grenoble, France, 2011.

[2] W. Bogdanich, "At V.A. hospital, a rogue cancer unit," *The New York Times,* 2009.

[3] R. J. Webster, N. J. Cowwan, G. S. Chirikjian and A. M. Okamura, "Nonholonomic modeling of needle steering," *Int. Journal of Robotic Research,* vol. 25, pp. 509-525, 2006.

[4] R. Seifabadi, I. Iordachita and G. Fichtinger, "Design of a teleoperated needle steering system for MRI-guided prostate interventions," in *Proc. of the Biomedical Robotics and Biomechatronics (BioRob)*, Rome, 2012.

[5] E. A. Dorileo, N. Hungr, N. Zemiti, C. Fouard and P. Poignet, "A modular CT/MRI-guided teleoperation platform for robot assisted punctures planning," in *28th CARS - Computer Assisted Radiology and Surgery*, Fukuoka, 2014.

[6] N. Zemiti, I. Bricault, C. Fouard, B. Sanchez and P. Cinquin, "LPR: A CT and MR-Compatible Puncture Robot to Enhance Accuracy and Safety of Image-Guided Interventions," *IEEE/ASME Transactions on Mechatronics,* vol. 13, no. 3, pp. 306-315, 2008.

[7] N. Hungr, C. Fouard, A. Robert, I. Bricault and P. Cinquin, "Interventional Radiology Robot for CT and MRI Guided Percutaneous Interventions," in *MICCAI*, Toronto, 2011.

[8] S. Misra, K. B. Reed, B. W. Shafer, K. T. Ramesh and A. M. Okamura, "Observations and Models for Needle-Tissue Interactions," in *Conf Proc IEEE Eng Med Biol Soc*, Kobe, Japan, 2009.

[9] N. Abolhassani, R. V. Patel and F. Ayazi, "Minimization of Needle Deflection in Robot-assisted Percutaneous Therapy," *The International Journal of Medical Robotics and Computer Assisted Surgery,* vol. 3, pp. 140-148, 2007.

[10] D. Glozman and M. Shoham, "Image-Guided Robotic Flexible Needle Steering," in *IEEE Transactions on Robotics, Vol 23, N.03*, 2007.

[11] Y. Kobayashi, A. Onishi, H. Watanabe, T. Hoshi, K. Kawamura and M. G. Fujie, "Developing a Planning Method for Straight Needle Insertion using Probability-Based Condition where a Puncture Occurs," in *IEEE International Conference on Robotics and Automation (ICRA)*, Kobe, Japan, 2009.

[12] E. Dehghan and S. Salcudean, "Needle Insertion Point and Orientation Optimization in Non-linear Tissue with Application to Brachytherapy," in *IEEE International Conference on Robotics and Automation (ICRA)*, Roma, Italy, 2007.

[13] M. Abayazid, M. Kemp and S. Misra, "3D flexible needle steering in soft-tissue phantoms using fiber bragg grating sensors," *In Proc. of ICRA - IEEE Int. Conf. on Rob. and Autom.,* pp. 5843-5849, 2013.

[14] S. Timoshenko and J. Gere, Mechanics of materials, New York: Van Nostrand Reinhold Co., 1972.

[15] Y. Mariappan, K. Glaser and R. Ehman, "Magnetic Resonance Elastography: A Review," *Clinical Anatomy,* vol. 23, no. 5, pp. 497-511, 2010.

[16] P. Hoskins and W. Svensson, "Current State of Ultrasound Elastography," *Ultrasound,* vol. 20, no. I, pp. 3-4, 2012.

[17] P. Schiavone, T. Boudou, E. Promayon, P. Perrier and Y. Payan, "A light sterilizable pipette device for the in vivo estimation of human," in *Conf Proc IEEE Eng Med Biol Soc*, 2008.

[18] S. M. LaValle, Planning Algorithms, University of Illinois: Ed. Cambridge, 2006.

[19] H. King, L. Cheng, P. Roan, D. Friedman, S. Kosari, D. Glozman, J. Rosen and B. Hannaford, "Raven II: Open platform for surgical robotics research," *IEEE Transactions on Biomedical Engineering,* vol. 60, no. 4, pp. 954-959, 2013.

[20] S. Daftry, M. Maurer, A. Wendel and H. Bischof, "Flexible and user-centric camera calibration using planar fiducial markers," in *Proceedings of the British Machine Vision Conference (BMVC)*, 2013.